



# CHORUS

This is the accepted manuscript made available via CHORUS. The article has been published as:

## Active thermal extraction of near-field thermal radiation

D. Ding, T. Kim, and A. J. Minnich

Phys. Rev. B **93**, 081402 — Published 2 February 2016

DOI: [10.1103/PhysRevB.93.081402](https://doi.org/10.1103/PhysRevB.93.081402)

# Active Thermal Extraction of Near-field Thermal Radiation

D. Ding,<sup>1</sup> T. Kim,<sup>1</sup> and A. J. Minnich<sup>1,\*</sup>

<sup>1</sup>*Division of Engineering and Applied Science,  
California Institute of Technology, Pasadena, California 91125, USA*

## Abstract

Radiative heat transport between materials supporting surface-phonon polaritons is greatly enhanced when the materials are placed at sub-wavelength separation as a result of the contribution of near-field surface modes. However, the enhancement is limited to small separations due to the evanescent decay of the surface waves. In this work, we propose and numerically demonstrate an active scheme to extract these modes to the far-field. Our approach exploits the monochromatic nature of near-field thermal radiation to drive a transition in a laser gain medium, which, when coupled with external optical pumping, allows the resonant surface mode to be emitted into the far-field. Our study demonstrates a new approach to manipulate thermal radiation that could find applications in thermal management.

Thermal radiation plays a role in many applications ranging from infrared detection and sensing applications for environmental and medical studies<sup>1,2</sup> to energy harvesting with solar thermophotovoltaics<sup>3-5</sup> and infrared emissions from Earth to space<sup>6</sup>. Thermal radiation is also essential to thermal management applications as in microelectronics<sup>7</sup>, space technology<sup>8</sup> and buildings<sup>9</sup>.

In the far-field, the blackbody limit governs the maximum radiative flux between two bodies. Recently, a number of works have demonstrated that near-field radiative heat transfer is enhanced by many orders of magnitude compared to the far-field limit for closely spaced objects with either natural<sup>10,11</sup> or engineered resonant surface modes<sup>12-16</sup>. There have also been efforts to couple these near-field modes into the far-field with the use of grating structures<sup>17</sup>, antennas<sup>18</sup>, and a thermal extraction lens<sup>19,20</sup>.

While these passive schemes modify the heat flux flowing from a hot object to a cool object, active schemes extract energy from a system through external work and allow an object to be cooled below the ambient temperature. In optics, external work in the form of laser light has been used to cool of gaseous matter to sub-millikelvin temperatures<sup>21,22</sup> by removing kinetic energy from the atoms. In solid-state materials, optical irradiation can also cool materials by emission of upconverted fluorescence<sup>23</sup> due to removal of energy in the form of phonons. This concept has been experimentally demonstrated to cool rare-earth doped glass<sup>24,25</sup> to cryogenic temperatures and recently to cool semiconductors by 40 K from the ambient temperature<sup>26</sup>. However, no active schemes have been proposed to extract energy out of a system as thermal radiation.

Here, we theoretically propose and numerically demonstrate an active thermal extraction scheme that extracts near-field thermal photons into the far-field. Our laser-based cooling approach exploits the monochromatic nature of near-field thermal radiation to drive a transition in a laser gain medium, which, when coupled with external optical pumping, allows the resonant surface mode to be emitted into the far-field. Our active scheme has an ideal efficiency that is orders of magnitude larger than that in traditional laser cooling of solids due to the relatively high energy of surface phonon polaritons compared to phonon energies. Furthermore, we show that the high energy density of monochromatic near-field thermal radiation is sufficient to pump transitions in gain media, a novel concept that could be used in other applications.

A schematic of the method is given in Fig. 1(a). A laser gain medium containing emitters

with discrete energy levels is placed in the near-field of a material that supports a resonant surface wave. We model the emitters as a three-level system, as shown in Fig. 1(b). An external pump laser is tuned to the 0-1 transition, exciting population into level 1. If the nearly-monochromatic thermal radiation drives the transition from 1-2 and the 2-0 transition is radiative with high quantum efficiency, the electron transition will emit blue-shifted photons in the far-field, thereby extracting the trapped near-field thermal radiation.

With a typical blackbody spectrum, the efficiency of such a scheme would be vanishingly small because of the low energy density and the broadband nature of thermal radiation<sup>27</sup>. However, in the near-field, it has been demonstrated that the radiative energy density is nearly monochromatic and far exceeds that in the far-field by several orders of magnitude<sup>28</sup>. Therefore, with near-field thermal radiation the 1-2 transition can be efficiently driven by matching the near-field energy resonance energy to the 1-2 transition energy.

To study this system, we use rate equations to determine the steady-state populations in each energy level with external and near-field pumping:

$$\frac{dN_2}{dt} = -W_{12}(N_2 - N_1) - \gamma_{12}N_2 - \gamma_{20}N_2 \quad (1)$$

$$\frac{dN_1}{dt} = W_{12}(N_2 - N_1) - W_{01}(N_1 - N_0) - \gamma_{10}N_1 + \gamma_{12}N_2 \quad (2)$$

$$\frac{dN_0}{dt} = W_{01}(N_1 - N_0) + \gamma_{20}N_2 + \gamma_{10}N_1 \quad (3)$$

$$N_t = N_0 + N_1 + N_2 \quad (4)$$

where  $W_{12}$  is the absorption rate of the 1-2 transition as a result of the near-field energy density,  $W_{01}$  is the absorption rate of the 0-1 transition due to external pumping,  $N_i$  are population density of each level,  $N_t$  is the total population density for system and  $\gamma_{ij}$  is the overall (radiative and non-radiative) spontaneous decay rate of the i-j transition. Here,  $\gamma_{ij}^r$  stands for radiative rate of the i-j transition such that  $\gamma_{ij} = \gamma_{ij}^r + \gamma_{ij}^{nr}$ . We assume that all energy levels are non-degenerate so that  $W_{ij} = W_{ji}$ . Solving Eqs. 1 to 4 in steady state yields the equilibrium population densities for each level from which the power density can

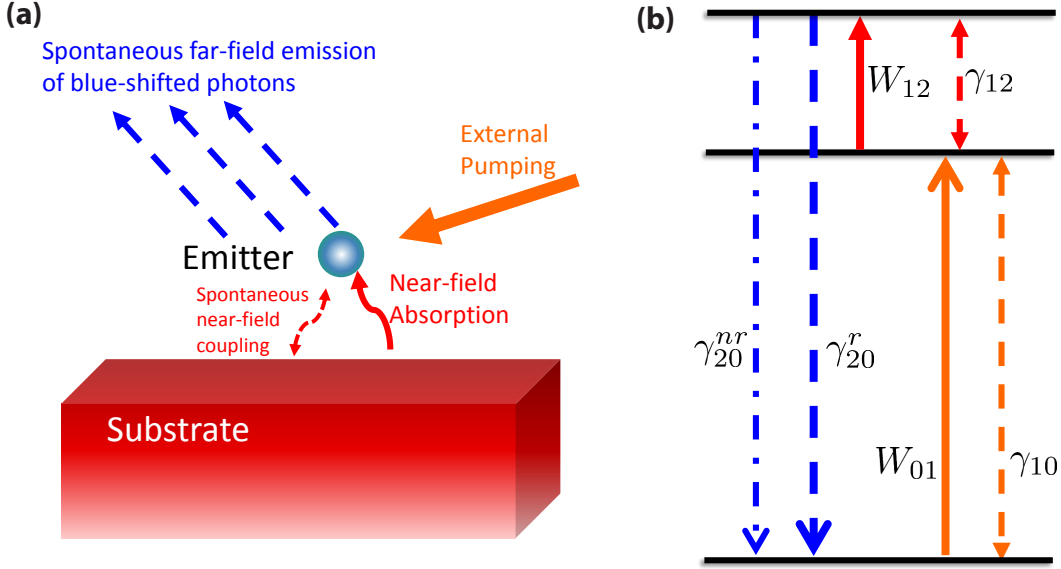


Figure 1. (a) Schematic of the active thermal extraction scheme. An emitter with discrete energy levels is placed in the near-field region of a semi-infinite planar substrate supporting a surface resonance. The external pumping couples with the near-field energy to be emitted as blue-shifted spontaneous emission in the far-field. (b) Energy level diagram of the emitter for our proposed concept. The 0-1 transition absorbs external pump photons, and near-field photons drive the 1-2 transition. Spontaneous emission from the 2-0 transition emits near-field photon to the far-field. The orange arrow indicates external optical pumping, the dashed arrows indicate various spontaneous decay channels with the blue arrows indicating the upconverted emitted photons carrying near-field energy into the far-field.

be expressed as

$$\begin{aligned}
 P_{01} &= \hbar\omega_{10}W_{01}(N_0 - N_1) \\
 &= \frac{\hbar\omega_{10}N_tW_{01}(W_{12}(\gamma_{10} + \gamma_{20}) + \gamma_{10}(\gamma_{12} + \gamma_{20}))}{W_{12}(\gamma_{10} + \gamma_{20}) + \gamma_{10}(\gamma_{20} + \gamma_{12}) + W_{01}(3W_{12} + 2(\gamma_{20} + \gamma_{12}))} \quad (5)
 \end{aligned}$$

$$\begin{aligned}
 P_{20,net} &= \hbar(\omega_{20} - \omega_{10})\gamma_{20}^r N_2 \\
 &= \frac{\hbar(\omega_{20} - \omega_{10})N_tW_{01}\gamma_{20}^r W_{12}}{W_{12}(\gamma_{10} + \gamma_{20}) + \gamma_{10}(\gamma_{20} + \gamma_{12}) + W_{01}(3W_{12} + 2(\gamma_{20} + \gamma_{12}))} \quad (6)
 \end{aligned}$$

where  $P_{01}$  is the external power density absorbed by the 0-1 transition and  $P_{20,net}$  is the net extracted power density into the far-field from the 2-0 transition.

Using Eqs. 5 and 6, the intrinsic efficiency of extraction can be expressed as the ratio of the amount of net extracted energy radiated into the far-field by the 2-0 transition with

respect to the external pump energy absorbed by the 0-1 transition

$$\eta_{10} = \frac{P_{20,net}}{P_{01}} = \frac{(\omega_{20} - \omega_{10})\gamma_{20}^r W_{12}}{\omega_{10}(W_{12}(\gamma_{20} + \gamma_{10}) + \gamma_{10}(\gamma_{20} + \gamma_{12}))} \quad (7)$$

In the ideal limit of a dominant radiative 2-0 transition  $\gamma_{20}$  and strong near-field absorption  $W_{12}$ , Eq. 7 tends towards  $(\omega_{20}/\omega_{10} - 1)(\gamma_{20}^r/\gamma_{20})$  which depends intuitively on the ratio of the emitted net energy and absorbed photon energy and on the radiative rate of the 2-0 transition for the photons that reach the far-field. When  $\eta_{10} > 0$ , there is net energy extracted from the system assuming no parasitic absorption of external pump energy. This assumption is reasonable as our pump wavelength is far from the resonance of the substrate such that the imaginary part of the permittivity is negligible. The intrinsic efficiency in Eq. 7 depends only on the internal parameters of the system and is independent of the absorption rate  $W_{01}$  of the external pumping (0-1) transition.

To estimate the efficiency of the scheme, we take properties based on rare-earth dopant embedded in gallium lanthanum sulfide (GLS) chalcogenide glass as the emitter system in the mid-infrared (MIR) region with typical values<sup>29,30</sup> listed in Table I. We remove the magnetic dipole contribution to the 2-0 transition by reducing the overall quantum efficiency from 93% to 79%. Here, we choose the wavelength-independent permittivity of the GLS chalcogenide glass<sup>31</sup> to be 4.8.

Transition	$\lambda(\mu\text{m})$	$\gamma_{ij}^0(\text{s}^{-1})$	QE (%)
0-1	1.83	1034	100
2-0	1.22	1370	79
1-2	3.88	36	100

Table I. Parameters of a typical rare-earth emitter in GLS chalcogenide glass for modeling our proposed system.  $\gamma_{ij}^0(\text{s}^{-1})$  stands for the decay rate of the i-j transition for an isolated emitter and QE is the quantum efficiency of the transition.

Then, we model the substrate permittivity with the expression  $\epsilon(\omega) = \epsilon_\infty(\omega_L^2 - \omega^2 - i\gamma\omega)/(\omega_T^2 - \omega^2 - i\gamma\omega)$  where  $\epsilon_\infty = 5.3$ ,  $\omega_T = 388.4 \times 10^{12} \text{ s}^{-1}$ ,  $\omega_L = 559.3 \times 10^{12} \text{ s}^{-1}$  and  $\gamma = 0.9 \times 10^{12} \text{ s}^{-1}$ . We tailor the substrate resonance to match the 1-2 transition with  $\text{Re}(\epsilon_{substrate}(\omega)) = -\epsilon_{medium}$  so as to enhance the energy density of the near-field thermal

radiation with the emitter<sup>32</sup>. Plasmonic resonances of the substrate in the MIR can be achieved with spoof plasmons in gold, for example<sup>33</sup>.

To calculate the intrinsic extraction efficiency of this system using Eq. 7, we need to know near-field absorption rate  $W_{12}$ . We use the formulation from Joulain et al.<sup>34</sup> to calculate the near-field energy density  $I(\omega)$  of the substrate<sup>32</sup> at 750 K where the blackbody spectrum peak matches the 1-2 transition wavelength in Table I. Then, we approximate the near-field absorption rate  $W_{12}$  using the isotropic stimulated rate in Eq. (29) of Archambault et al.<sup>35</sup>. We incorporate the energy per unit volume  $I(\omega) = \int_0^\infty I(\omega, k)dk$  in Fig. 2(a) for the transition for different values of wave vector  $k$  to obtain

$$W_{ij, near-field} = \frac{\gamma_{ij}^0 \pi^2 c^3}{2\hbar\omega_0^3} \int_{-\infty}^{\infty} \int_0^{\infty} \left(1 + \left| \frac{k}{\sqrt{\epsilon_{medium} - k^2}} \right|^2\right) I(|\omega|, k) g(\omega) dk d\omega \quad (8)$$

$$g(\omega) = \frac{\frac{\Delta\omega}{2\pi}}{(\omega - \omega_0)^2 + (\Delta\omega/2)^2} \quad (9)$$

where  $\gamma_{ij}^0$  is the spontaneous decay rate for an isolated emitter and  $g(\omega)$  is the lineshape of the transition<sup>32</sup> with a linewidth of  $\Delta\omega$ . The distance dependence of  $\gamma_{ij}$  of an isotropic emitter due to the modification of density of states by the surface in the near-field follows the formulation in Chance et al.<sup>36</sup>.

The induced absorption rate  $W_{01}$  due to far-field pumping is calculated using the well-known expression for the stimulated rate<sup>37</sup>  $W_{ij, external} = (\lambda^2 g(\omega) I_v \gamma_{ij}^r) / (8\pi n^2 \hbar \omega)$  where  $\gamma_{ij}^r$  is the radiative spontaneous decay rate that couples to external pumping from the far-field,  $I_v$  is the incident intensity of the external pumping field and  $n$  is the index of the chalcogenide medium. The linewidth for the 0-1 and 2-1 transitions are assumed to be  $2 \times 10^{11} \text{ s}^{-1}$ , comparable to those of typical laser gain media<sup>37</sup>.

The intrinsic efficiency of thermal extraction versus distance from the emitter is shown in Fig. 2(a). The maximum efficiency is small, around 4% and decreases to zero beyond a few hundred nanometers. The total extracted intensity is defined as the integral of the power emitted by the 2-0 transition over all distances,  $\int_{z_1}^{z_2} P_{20, net} dz$ . We integrate from  $z_1 = 10 \text{ nm}$  onward until the intrinsic efficiency decreases to almost zero. Figure 2(b) shows the extracted power per unit area as a function of input power  $I_v$ . The extracted power increases linearly with the input power for low power inputs before saturating at higher powers, but the overall power extracted is orders of magnitude lower than the input power. A limiting case of Eq. 6 can be found for large  $W_{01}$  as  $\hbar(\omega_{20} - \omega_{10})W_{12}\gamma_{20}^r N_t / (3W_{12} + 2(\gamma_{20} + \gamma_{12}))$ . Integrating this limit over distance agrees with the saturation curve as plotted in Fig. 2(b).

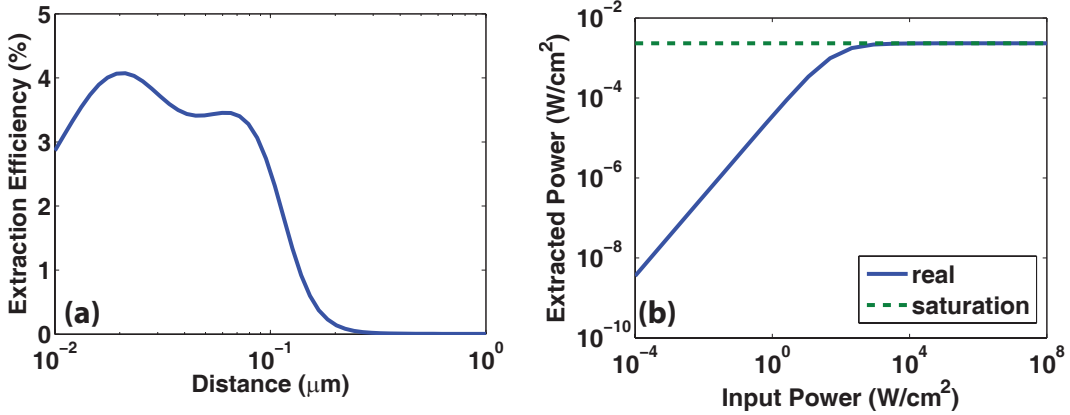


Figure 2. (a) Extraction efficiency  $\eta_{10}$  of external pumping from the 0-1 transition assuming properties in Table I. The low efficiency in the blue line is a result of the large spontaneous rate for 1-2 transition in the near-field in Fig.3(a). (b) Integrated power extracted for emitters uniformly distributed from surface. The density of emitters is assumed to be  $10^{20} \text{ cm}^{-3}$ . The saturation behavior approaches the green dashed "saturation" line due to the finite number of emitters in the system saturating the population difference at high input powers.

Figure 2 shows that active thermal extraction is possible, but both the intrinsic efficiency and the total power extracted are very small for the chosen parameters. However, according to the limit of Eq.7, the maximum efficiency should be around 35%, much higher than in the example. To understand the reason for this difference, we examine Eq.7 in more detail. The maximum efficiency occurs when  $\gamma_{20}$  and  $W_{12}$  are large. We calculate the transition rates versus distance from the substrate in Fig.3(a), and observe that the transition rates for 0-1 and 2-0 transitions are not affected by the presence of a surface as they are off-resonant. However, the decay rate for the 1-2 transition  $\gamma_{12}$  is strongly enhanced as the emitter approaches the surface<sup>36,38,39</sup>. As a result, the near-field absorption rate is smaller by about two orders of magnitude compared to the decay rate even though both are enhanced by orders of magnitude due to the increase in the optical density of states in the near-field. Physically, this calculation indicates that as electrons are excited from energy level 1 to 2, they immediately decay back to level 1 at the rate  $\gamma_{12}$ .

The reason for this cycling is that the thermal near-field energy density is not sufficient to allow near-field absorption to dominate over near-field spontaneous decay. Archambault et al.<sup>35</sup> also highlight the need for some minimum energy density for stimulated emission to

dominate spontaneous decay. Unlike the case for stimulated emission of surface plasmons with external pumping<sup>40-42</sup> where the external laser field intensities can be tuned, here the thermal energy density is restricted to that for a blackbody. Thus, the spontaneous decay rate will always dominate over near-field absorption for realistic values of near-field energy density. On the other hand, Fig. 2(a) also shows that while a resonantly enhanced  $\gamma_{12}$  offsets the enhanced absorption  $W_{12}$ , the extraction efficiency  $\eta_{10}$  still requires a large value of  $W_{12}$ . Beyond a emitter-substrate distance of about 100 nm, the extraction efficiency in Fig. 2(a) drops significantly as a result of the low near-field energy density, although the ratio  $W_{12}/\gamma_{12}$  remains of the same order of magnitude up to 1  $\mu\text{m}$ .

Therefore, to break the cycling between levels 1 and 2, it is essential that the strongly radiative decay rate from 2-0 ( $\gamma_{20}$ ) is comparable to the decay rate  $\gamma_{12}$  in the near-field. Figure 3(b) shows that the efficiency is boosted to almost the ideal limit at short distances if  $\gamma_{20}$  is increased substantially. In Eq. 7, if we increase  $\gamma_{20}$  to be more comparable to  $\gamma_{12}$  in the near-field, then the ratio of  $\gamma_{20}^r/\gamma_{20}$  begins to dominate in the expression, increasing the extraction efficiency towards the ideal limit discussed earlier.

The factors discussed above affect the intrinsic efficiency, but the total extracted power also depends on the input power  $W_{01}$  and the emitter density  $N_t$ . Firstly, the absorption of the pump power  $W_{01}$  depends on the linewidth of the 0-1 transition, and decreasing the linewidth increases  $W_{01}$  in Eq. 6 due to the increased concentration of input power in a given bandwidth for each emitter. The pump absorption could also be increased by photon recycling as in traditional laser cooling of solids, but we do not account for this possibility here. Secondly, the total dopant density  $N_t$  also affects the extracted power. As discussed earlier, the saturation limit at higher incident powers is proportional to the dopant density, and therefore the dopant density must increase to increase the saturation limit.

Using this understanding, we now recalculate the efficiency and extracted power for an optimized gain medium with the spontaneous rate for the 2-0 transition increased to  $1.37 \times 10^7 \text{ s}^{-1}$ ,  $\Delta\omega_{10} = 2 \times 10^9 \text{ s}^{-1}$  and  $N_t = 10^{21} \text{ cm}^{-3}$ . Figure 3(c) shows that the intrinsic extraction efficiency is much higher than in Fig. 2(a) and almost near the ideal limit for small emitter-substrate distances. The decrease of efficiency at larger emitter-substrate distances is due to a decrease in near-field coupling. Figure 3(d) shows a much-increased integrated extracted power at each given input power compared to Fig. 2(b). The saturation limit derived earlier also agrees with the full calculation at higher input powers.

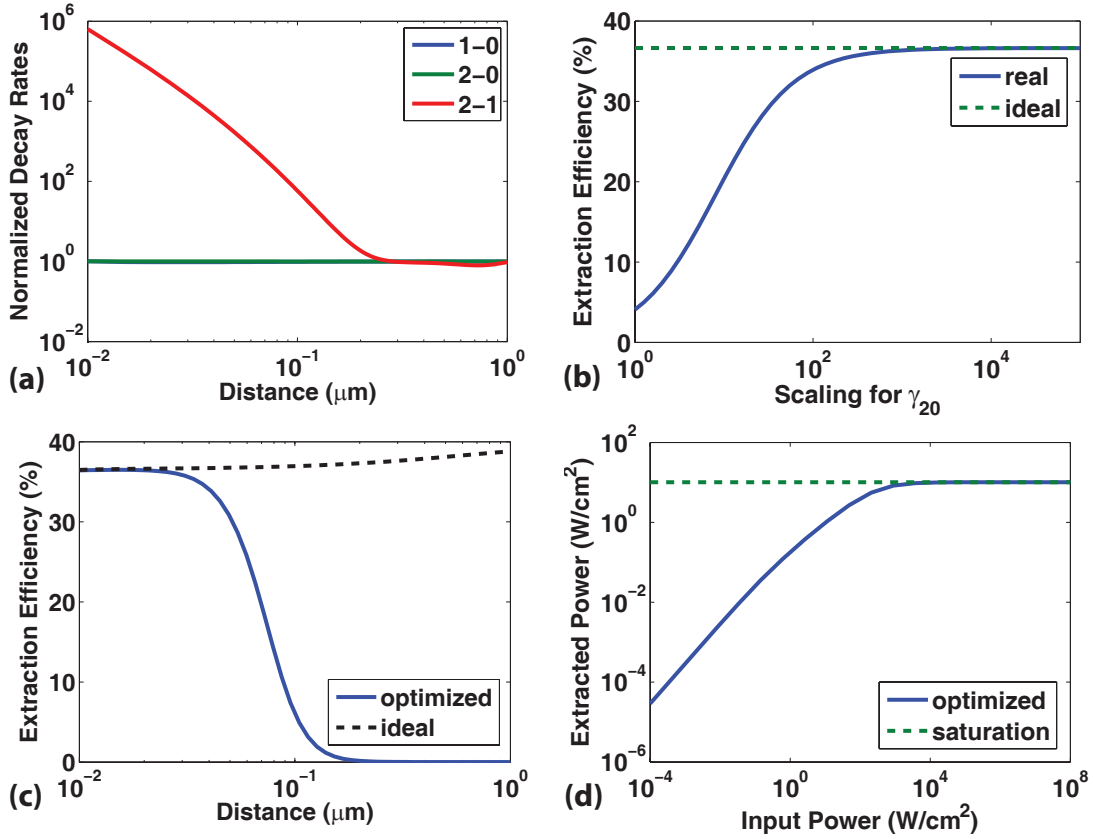


Figure 3. (a) Normalized spontaneous decay rates versus distance for three different transitions. The 2-1 transition is on resonance with the substrate dispersion and is enhanced greatly whereas the 0-1 and 2-0 transitions are not significantly affected by the presence of the substrate. (b) Intrinsic extraction efficiency  $\eta_{10}$  versus the scaling of the spontaneous rate  $\gamma_{20}$  at  $d = 20$  nm. The blue line shows real behavior according to Eq. 7. Increasing  $\gamma_{20}$  greatly enhances the efficiency so that it approaches the ideal limit of the system. (c) Intrinsic extraction efficiency versus emitter-substrate distance for an optimized system. The extraction efficiency follows the ideal limit for small distances before decreasing due to a decreasing  $W_{12}$  and is much improved compared to Fig. 2(a). (d) Integrated power extracted of the optimized system with emitters uniformly distributed from the substrate surface. An increased pump absorption and a higher emitter density lead to a much higher saturation limit shown as the dashed line.

This calculation shows that the active thermal extraction scheme has potential to efficiently extract a significant amount of near-field thermal radiative energy. The key to realizing this potential is to identify an appropriate emitter with a surface resonance and

a gain medium with matching transitions in the mid-infrared wavelength range where photons are thermally populated at typical temperatures. Additionally, recycling the pump photons to increase absorption, as is done in traditional laser cooling of solids, is important to decrease the required pump power. A high dopant density is still required to increase the saturation limit. Cerium doped crystals can potentially be a candidate as they have a  $4f^05d^1 \rightarrow 4f^15d^0$  transition with a short lifetime<sup>43</sup> of around 40 ns, ideal for the 2-0 transition proposed here, as well as a mid-infrared transition<sup>43</sup> of 4.5  $\mu\text{m}$  for the near-field absorption.

Our work shares some similarities with laser cooling of solids<sup>24–26,44</sup> and active schemes in plasmonics<sup>40,41,45</sup>, photonic crystals<sup>46</sup>, and metamaterials<sup>47,48</sup> but differs in a number of important ways. First, laser cooling directly extracts phonons, while our scheme extracts surface phonon polaritons. Therefore, our scheme has potential to be much more efficient than laser cooling because of the significantly higher energy of surface phonon polaritons than phonons. For instance, the ideal efficiency of laser cooling of solids is typically a few percent<sup>24–26</sup> while our ideal efficiency is 50% for the chosen wavelengths if the 2-0 transition has unity quantum efficiency. Further reduction in the pump fluence can be made by optimizing pump recycling. Also, laser cooling requires the medium to be cooled to possess very specific energy levels, whereas our scheme only requires that the medium possess a surface resonance.

The most important difference between this work and prior works on near-field coupling and gain media<sup>40–42,45</sup> is that in the present work, the atomic transition is pumped by a near-field thermal radiative source rather than a coherent pump. Unlike typical broadband radiation in the far-field, the nearly monochromatic nature of near-field thermal radiation allows atomic transitions to be efficiently driven, a concept that could be used for other photonics applications. However, although the near-field energy density is high compared to that in the far-field, it is not sufficient to cause the imaginary part of permittivity of the gain medium to become positive; our medium is actually absorptive under all conditions. Our approach does not lead to any form of stimulated emission or coherent single mode emission and thus is distinctly different from active schemes in plasmonics used to realize spasers<sup>40–42,45</sup> or to compensate loss<sup>47,48</sup>.

In conclusion, we have numerically demonstrated an active thermal extraction scheme that allows bound surface waves to be converted from evanescent to propagating waves.

Our laser-based cooling approach exploits the monochromatic nature of near-field radiation to drive a transition in a gain medium simultaneously with an external pump, thereby extracting near-field energy to the far-field. Our work demonstrates the large potential for manipulating thermal radiation using active processes rather than the traditional passive approaches.

## ACKNOWLEDGMENTS

This work is part of the 'Light-Material Interactions in Energy Conversion' Energy Frontier Research Center funded by the U.S. Department of Energy, Office of Science, Office of Basic Energy Sciences under Award Number DE-SC0001293. D.D. gratefully acknowledges the support by the Agency for Science, Technology and Research (Singapore). T. K. acknowledges the support by the Jeongsong Cultural Foundation (South Korea). A. J. M. acknowledges the support of the Northrop Grumman Corporation.

---

\* aminnich@caltech.edu

- <sup>1</sup> D. N. Kendall, *Applied Infrared Spectroscopy*, 1st ed. (Reinhold Publishing Corp. 1966., 1966).
- <sup>2</sup> P. Werle, F. Slemr, K. Maurer, R. Kormann, R. Mücke, and B. Jänker, *Optics and lasers in engineering* **37**, 101 (2002).
- <sup>3</sup> R. M. Swanson, *Proceedings of the IEEE* **67**, 446 (1979).
- <sup>4</sup> P. Bermel, M. Ghebrebrhan, M. Harradon, Y. X. Yeng, I. Celanović, J. D. Joannopoulos, and M. Soljačić, *Nanoscale Research Letters* **6**, 549 (2011).
- <sup>5</sup> A. Lenert, D. M. Bierman, Y. Nam, W. R. Chan, I. Celanović, M. Soljačić, and E. N. Wang, *Nat Nano* **9**, 126 (2014).
- <sup>6</sup> S. J. Byrnes, R. Blanchard, and F. Capasso, *PNAS* **111**, 3927 (2014).
- <sup>7</sup> L. Buller and B. McNelis, *IEEE Transactions on Components, Hybrids, and Manufacturing Technology* **11**, 538 (1988).
- <sup>8</sup> J. Jenness, *Proceedings of the IRE* **48**, 641 (1960).
- <sup>9</sup> A. P. Raman, M. A. Anoma, L. Zhu, E. Rephaeli, and S. Fan, *Nature* **515**, 540 (2014).
- <sup>10</sup> S. Shen, A. Narayanaswamy, and G. Chen, *Nano Lett.* **9**, 2909 (2009).

- <sup>11</sup> E. Rousseau, A. Siria, G. Jourdan, S. Volz, F. Comin, J. Chevrier, and J.-J. Greffet, *Nat Photon* **3**, 514 (2009).
- <sup>12</sup> A. W. Rodriguez, O. Ilic, P. Bermel, I. Celanović, J. D. Joannopoulos, M. Soljačić, and S. G. Johnson, *Phys. Rev. Lett.* **107**, 114302 (2011).
- <sup>13</sup> S.-A. Biehs, M. Tschikin, and P. Ben-Abdallah, *Phys. Rev. Lett.* **109**, 104301 (2012).
- <sup>14</sup> Y. Guo and Z. Jacob, *Opt. Express* **21**, 15014 (2013).
- <sup>15</sup> O. D. Miller, S. G. Johnson, and A. W. Rodriguez, *Phys. Rev. Lett.* **112**, 157402 (2014).
- <sup>16</sup> J. Shi, B. Liu, P. Li, L. Y. Ng, and S. Shen, *Nano Lett.* **15**, 1217 (2015).
- <sup>17</sup> J.-J. Greffet, R. Carminati, K. Joulain, J.-P. Mulet, S. Mainguy, and Y. Chen, *Nature* **416**, 61 (2002).
- <sup>18</sup> J. A. Schuller, T. Taubner, and M. L. Brongersma, *Nat Photon* **3**, 658 (2009).
- <sup>19</sup> Z. Yu, N. P. Sergeant, T. Skauli, G. Zhang, H. Wang, and S. Fan, *Nat Commun* **4**, 1730 (2013).
- <sup>20</sup> C. Simovski, S. Maslovski, I. Nefedov, S. Kosulnikov, P. Belov, and S. Tretyakov, *Phot. Nano. Fund. Appl.* **13**, 31 (2015).
- <sup>21</sup> T. W. Hänsch and A. L. Schawlow, *Optics Communications* **13**, 68 (1975).
- <sup>22</sup> W. D. Phillips, *Rev. Mod. Phys.* **70**, 721 (1998).
- <sup>23</sup> P. Pringsheim, *Z. Physik* **57**, 739 (1929).
- <sup>24</sup> M. Sheik-Bahae and R. I. Epstein, *Nat Photon* **1**, 693 (2007).
- <sup>25</sup> D. V. Seletskiy, S. D. Melgaard, S. Bigotta, A. Di Lieto, M. Tonelli, and M. Sheik-Bahae, *Nat Photon* **4**, 161 (2010).
- <sup>26</sup> J. Zhang, D. Li, R. Chen, and Q. Xiong, *Nature* **493**, 504 (2013).
- <sup>27</sup> A. E. Siegman, *Lasers*, new ed. (University Science Books, Mill Valley, Calif., 1986).
- <sup>28</sup> A. V. Shchegrov, K. Joulain, R. Carminati, and J.-J. Greffet, *Phys. Rev. Lett.* **85**, 1548 (2000).
- <sup>29</sup> T. Schweizer, B. N. Samson, J. R. Hector, W. S. Brocklesby, D. W. Hewak, and D. N. Payne, *J. Opt. Soc. Am. B* **16**, 308 (1999).
- <sup>30</sup> A. B. Seddon, Z. Tang, D. Furniss, S. Sujecki, and T. M. Benson, *Opt. Express* **18**, 26704 (2010).
- <sup>31</sup> H. Yayama, S. Fujino, K. Morinaga, H. Takebe, D. W. Hewak, and D. N. Payne, *Journal of Non-Crystalline Solids* **239**, 187 (1998).
- <sup>32</sup> See Supplemental Material for derivation of Eq. (8) and plot of near-field energy vs. frequency for different distances from the substrate.

- <sup>33</sup> R. Stanley, *Nat Photon* **6**, 409 (2012).
- <sup>34</sup> K. Joulain, J.-P. Mulet, F. Marquier, R. Carminati, and J.-J. Greffet, *Surface Science Reports* **57**, 59 (2005).
- <sup>35</sup> A. Archambault, F. Marquier, J.-J. Greffet, and C. Arnold, *Phys. Rev. B* **82**, 035411 (2010).
- <sup>36</sup> R. R. Chance, A. Prock, and R. Silbey, in *Advances in Chemical Physics*, edited by I. Prigogine and S. A. Rice (John Wiley & Sons, Inc., 1978) pp. 1–65.
- <sup>37</sup> A. Yariv, *Quantum Electronics*, 3rd ed. (Wiley, New York, 1989).
- <sup>38</sup> K. T. Shimizu, W. K. Woo, B. R. Fisher, H. J. Eisler, and M. G. Bawendi, *Phys. Rev. Lett.* **89**, 117401 (2002).
- <sup>39</sup> K. Okamoto, I. Niki, A. Shvartser, Y. Narukawa, T. Mukai, and A. Scherer, *Nat Mater* **3**, 601 (2004).
- <sup>40</sup> J. Seidel, S. Grafström, and L. Eng, *Phys. Rev. Lett.* **94**, 177401 (2005).
- <sup>41</sup> M. A. Noginov, G. Zhu, M. Bahoura, J. Adegoke, C. E. Small, B. A. Ritzo, V. P. Drachev, and V. M. Shalaev, *Opt. Lett.* **31**, 3022 (2006).
- <sup>42</sup> M. A. Noginov, G. Zhu, A. M. Belgrave, R. Bakker, V. M. Shalaev, E. E. Narimanov, S. Stout, E. Herz, T. Suteewong, and U. Wiesner, *Nature* **460**, 1110 (2009).
- <sup>43</sup> E.-G. Scharmer, M. Leiss, and G. Huber, *J. Phys. C: Solid State Phys.* **15**, 1071 (1982).
- <sup>44</sup> J. B. Khurgin, *Phys. Rev. Lett.* **98**, 177401 (2007).
- <sup>45</sup> J. Cuerda, F. Rütting, F. J. García-Vidal, and J. Bravo-Abad, *Phys. Rev. B* **91**, 041118 (2015).
- <sup>46</sup> P. Bermel, E. Lidorikis, Y. Fink, and J. D. Joannopoulos, *Phys. Rev. B* **73**, 165125 (2006).
- <sup>47</sup> S. Wuestner, A. Pusch, K. L. Tsakmakidis, J. M. Hamm, and O. Hess, *Phys. Rev. Lett.* **105**, 127401 (2010).
- <sup>48</sup> X. Ni, S. Ishii, M. D. Thoreson, V. M. Shalaev, S. Han, S. Lee, and A. V. Kildishev, *Opt. Express* **19**, 25242 (2011).